Chalcogenide Letters Vol. 18, No. 11, November 2021, p. 725 - 733

Effect of surface modification and exfoliation of molybdenum disulfide for application in batteries and supercapacitors

M. Subitha*, B. Bindhu
Department of Physics, Noorul Islam Centre for Higher Education, Kumaracoil, Thuckalay- 629 180, Tamilnadu, India

Molybdenum disulfide (MoS_2) flakes, a semiconductor-like material having high surface area and versatile electronic structure finds application in numerous electrochemical energy storage devices. Boosting its surface properties improves the overall storage performance to a greater extent. This present research work focuses on the surface modification of MoS_2 using Lithium stearate ($LiC_{18}H_{35}O_2$). The $LiC_{18}H_{35}O_2$ modification supports lithium intercalation between the layers of MoS_2 thereby facilitating the exfoliation process and simultaneous modification of the flakes. The resultant samples were characterized using X-ray powder diffraction (XRD), Raman spectroscopy, Fourier-transform infrared (FTIR) spectroscopy, Thermogravimetric analysis (TGA), Scanning electron microscopy (SEM) and Energy dispersive x-ray (EDAX) analysis. EDAX results revealed that the stearate surface treated MoS_2 samples exhibited larger increase in Carbon and Oxygen elemental concentrations, which further confirms modification. The modifier and the material itself have good lubricant properties suggesting lithium stearate assisted modification and exfoliation of MoS_2 as a better choice to make composites with enhanced electrical and chemical properties suitable for energy storage applications in batteries and supercapacitors.

(Received August 25, 2021; Accepted November 18, 2021)

Keywords: Nanomaterials, Molybdenum disulfide, Lithium stearate, Surface modification, Lipophilic property, Exfoliation, XRD, FTIR, TGA, SEM, EDAX, Electrochemical energy storage, Battery, Supercapacitor, Electronic application

1. Introduction

Nano, this word fills almost all applications in the world and has gained much more attention because of its uniqueness. In earlier days, bulk materials are commonly used for real-world applications. The nanomaterials conventionally evolved out of these bulk counterparts [1]. However, such nanomaterials have shown more promising results when compared to the bulk materials which were used earlier. Moreover, these materials consist of several particles with high level properties, even the single material has multi-phases. Nanomaterials are classified according to the mode of construction. Molybdenum disulphide (MoS_2) which belongs to the family of Transition metal dichalcogenide (TMDs) has gathered much more attention in the past decade because of its unique properties. There are several properties that make them find applicable in different fields including Electrocatalytic hydrogen evolution (HER), Field effect transistor (FET), Optical electronic devices, Lithium batteries, Biosensors, Solar photovoltaic cells, etc. MoS_2 nanosheets normally exhibits increased electrical [2,3], physicochemical [4,5] and mechanical [6,7,8] properties when compared with its counterparts.

Electrochemical energy storage devices like batteries, supercapacitors, etc., find wider applications in real life. So as to fulfill the necessities of almost every electronic application that consumes higher energy, formulating low-cost electrochemical storage materials is an increasing need of the hour. Generally, in the process of developing effective electrochemical materials, nanomaterials play a significant role. Therefore, the development of high energy density material composites is being considered as one of the major technological challenges.

* Corresponding author: mahesubi2014@gmail.com
https://doi.org/10.15251/CL.2021.1811.725

In addition to higher energy density, the availability of low-cost materials for producing these storage devices was considered as another major challenge. The conventionally available elements like magnesium, sodium, calcium, aluminum, potassium, lithium, etc., take an essential part in formulating these electrochemical storage devices with high energy density. Recent advancements in nanomaterials have successfully enhanced the production of chemically-stable energy storage devices to a wider extent that, too with increased lifetime and enhanced durability in these storage devices.

Presently, the conventionally used energy storage devices include Lithium-ion (Li-ion) batteries possessing dissimilar physically and chemically varied electrode materials including Nickel cobalt aluminium (Ni-Co-Al) oxides, Lithium-titanate (Li-Ti) oxides, etc. Conversely, for enhancing the storage capabilities in these functional nanomaterials, formulation of novel and superior materials with diverse features are typically needed. So as to fulfill the aforementioned requirements, in this paper, Lithium stearate was considered as the functional nanomaterial to be used for this experiment.

Lithium stearate is a compound which is formally categorized as soap. It has several distinctive properties that make it feasible in wide range of applications. Lithium stearate has properties that act as a lubricant and have numerous other properties as well. Lithium stearate as a surface modifier for MoS_2 flakes is experimented herein for the first time with the primary objective of improving the dispersibility and electrical properties of the flakes. Here, several methods were adopted that includes Chemical exfoliation, Hydrothermal synthesis and Chemical vapor deposition for the synthesis of nanoflakes [9]. This present research work offers a comparative analysis over the existing bulk materials and the novel exfoliated samples with modified samples. The respective samples were coded as M1, M2 and M3. The property changes in these M1, M2 and M3 samples were subsequently examined.

This paper was summarized as follows. A detailed introduction to nanomaterials, and particularly, the distinctive properties and applications of molybdenum disulphide for electrochemical energy storage was discussed in Section 1. The materials and methods including Preparation of MoS_2 flakes, Preparation of lithium stearate, and Surface modification using lithium stearate were elaborated in Section 2. The characterization of the prepared samples in terms of different techniques like XRD analysis, Raman spectroscopic analysis, TG-DTA process and SEM analysis were explained in Section 3. The results and discussions highlighting the unique features of the produced samples using XRD analysis, FTIR analysis, TGA analysis and SEM EDAX analysis were given in Section 4. The concluding remarks on how MoS_2 was effectively exfoliated and modified using lithium stearate as a novel modifier, and its related applications in electrochemical energy storage devices were summarized in Section 5.

2. Materials and Methods

2.1. Materials

Molybdenum disulphide (MoS_2, 99% Pure) with molecular weight 160.06 g/mol of AR grade was taken for analysis. Stearic acid molecular weight (M.W., 284.49 g/mol) and Lithium hydroxide having M.W. of 41.96 g/mol and Dimethylformamide (DMF, purity ≥ 99.9%) were used for this analysis.

2.2. Preparation of MoS_2 flakes

100 ml of distilled water was added to 1 mol of bulk MoS_2 (M1) and stirred for about 30 minutes to make a perfect mixture. The resultant mixture was then probe sonicated (PCI Analytics PS120W, 20 kHz) for 30 minutes. The supernatant solution was removed and kept in a beaker. Sonication resulted in shear forces, arising from the collapse of cavitation bubbles that shall peel of the layers [10]. This separated solution was subjected to centrifuging and the exfoliated MoS_2 samples were collected, washed and then placed in an oven at 60^0C for about 12 hours [11,12]. The final samples collected were coded as M2.

2.3. Preparation of Lithium stearate

Lithium stearate was prepared by combining stearic acid and lithium hydroxide. Stearic acid of required quantity is dissolved with dimethylformamide. Proportionate quantity of Lithium hydroxide is dissolved separately in distilled water. These two solutions were mixed well and then stirred for 30 minutes. The samples were then dried in an oven. The dried material, Lithium stearate is used as surface modifier in this present research.

2.4. Surface modification

The sample M2 was then surface modified using Lithium stearate by chemical method. The modification process is done by adding 50 ml of distilled water with exfoliated MoS_2 (M2) in the ratio of (1:1). This mixture is stirred well and sonicated using probe sonicator for 30 minutes.

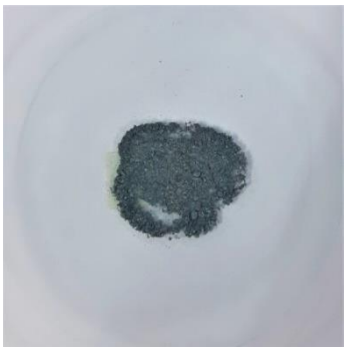

Fig. 1. Photography of the Surface modified MoS_2 sample (M3).

The solution was then oven dried for 18 hours [13]. The modified sample (M3) was thus obtained. Further, these three samples M1, M2, M3 were considered for different characterization for comparative studies [14,15]. The as-formed surface modified MoS_2 sample M3 is shown in Fig. 1.

3. Characterization

XRD studies were done using Philips X-Pert Pro. The incident X-rays (λ 1.54 A0) from the Cu-target were monochromatized using a Ni filter. XRD patterns were recorded with a step scan with step size of 0.02 between 50 and 700 (2^{θ}). Raman spectroscopic analysis was carried out using a HR 800 micro-Raman (HORIBA Jobin Yovon, France) for bulk (M1), exfoliated (M2) and modified (M3) MoS_2 samples in the scanning range of 250-500 cm^{-1} with an incident laser of excitation wavelength 514 nm.

TG-DTA process was performed using TA instrument (Q50) V20.13 Build 39, (USA) at room temperature for analysis at 80^0C. FTIR spectra were obtained in the range of 550–4000 cm^{-1} by BRUKER Alpha T, Germany. SEM analysis was carried out using FEG-SEM (JSM-7600F, Japan) with an accelerating voltage of 10 kV. To prepare the samples for SEM analysis, a small quantity of bulk (M1), exfoliated (M2) and modified (M3) MoS_2 samples were used in this experiment.

4. Results and discussions

4.1. XRD Analysis

Fig.2 depicts the XRD spectra of M1, M2 and M3 samples. The characteristic diffraction peaks of (002), (100), (103), (105) and (110) for sample M1 at 2θ position 14^0,

33^0, 40^0, 50^0, 59^0 according to JCPDS card no: 37-1492 confirms the hexagonal phase MoS_2 [16].

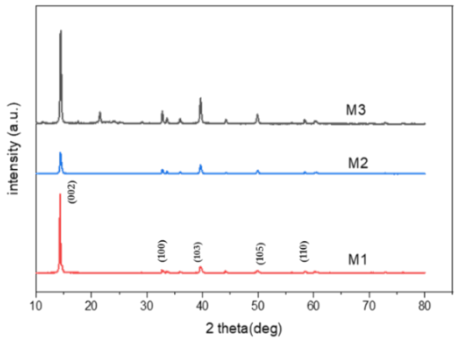

Fig. 2. XRD spectra of Bulk (M1), Exfoliated (M2) and Modified (M3) samples of MoS_2.

The well-defined sharp peaks signify the crystallinity of the sample. On comparing the diffraction peaks of sample M1 with that of M2, it was clearly observed that, the (002) peak intensity got reduced which corresponds to the de-staking of MoS_2 layers. This decreased intensity suggests the reduction of MoS_2 layer thickness.

The intense (103) peak indicates the in-layer crystallinity of sample M2. For sample M3, all the peak intensities got increased to a greater extent signifying improved crystallinity, and an additional peak at 210 which might be attributed to the cluster formation. The lattice parameters were calculated using equation 1 as given below,

$$\frac{1}{d_{hkl}^2} = \frac{4}{3}\left(\frac{h^2hk^2k^2}{a^2}\right) + \left(\frac{1}{c}\right)^2 \quad (1)$$

where, d signifies the inter-planar spacing, and h, k, l corresponds to the miller indices.

The calculated lattice parameters of M1, M2, M3 samples were shown in Table 1. Hence, the calculated lattice parameters were found to be in agreement with the standard JCPDS data. The calculated values showed minor decrease in exfoliated (M2) and modified (M3) samples. This might be attributed due to the increase in stress.

Table 1. Calculated lattice parameters of M1, M2, M3 samples.

Samples	**Lattice parameters**	
	Standard value (Å)	**Calculated value (Å)**
M1	a = b = 3.161 c = 12.299	a = b = 3.154 c = 12.314
M2		a = b = 3.15 c = 12.259
M3		a = b = 3.154 c = 12.232

The average crystalline size (D) of M1, M2 and M3 samples were calculated using equation 2 as given below,

$$D = \frac{kl}{b\cos q} \quad (2)$$

Where, D corresponds to the average crystalline size, k represents the shape factor (0.94), λ corresponds to the wavelength of X-ray used (1.540569 A˚), β represents the full width at half maximum, and θ represents the diffraction angle.

Accordingly, the micro strain (ε) of the material was calculated as per equation 3 that could be mathematically expressed as,

$$e = \frac{b \cos q}{4} \tag{3}$$

4.1.1. Williamson-Hall (W-H) Plot

Table 2 represents the calculated crystalline parameters of M1, M2, M3 samples, and was clearly seen that, the crystalline size decreases for M1 which was due to the increase in broadening owing to increase in crystalline size.

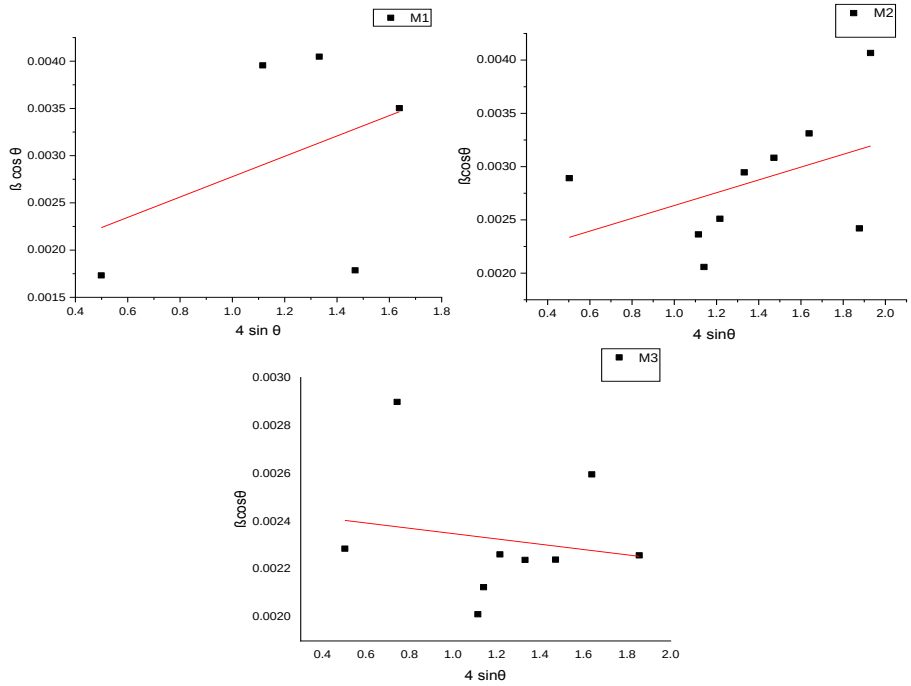

Fig. 3. Williamson-Hall Plot for M1, M2 and M3 samples.

Table 2. Calculated crystalline parameters for M1, M2 and M3 samples.

Samples	Average crystalline size (D)		Lattice strain (ε)	
	Calculated value (nm)	W-H plot (nm)	Calculated value × 10^{-3}	W-H Plot × 10^{-3}
M1	82.32	81.56	0.374	1.08
M2	49.88	68.30	0.689	0.6
M3	62.35	56.36	0.528	0.11

On adding modifier, the size increases and the stress decreases. It could be clearly seen that, the average crystalline size decreases with exfoliation. The value remains the lowest for M2. This change in crystalline size is the typical characteristics of exhibiting better exfoliation. **Fig.3.,** displays the Williamson-Hall plot for M1, M2 and M3 MoS_2 samples.

4.2. FTIR Analysis

To investigate the MoS_2 surface functionalization, FTIR analysis was performed for all the three samples M1, M2 and M3, and the corresponding results were shown in Fig. 4. The FTIR spectra of M1 match well with the reported data for bulk MoS_2. The spectra of M2 shows peaks at 1604 cm^{-1}, 1232 cm^{-1}, 860 $cm^{-1}$and 626 cm^{-1}. The band 920 cm^{-1} is due to the S-S bond [17]. M3 shows the peaks. The spectra of sample M3 showed the appearance of intense peaks at 2915 cm^{-1} and 2848 cm^{-1} representing the C-H and C-O bonds respectively.

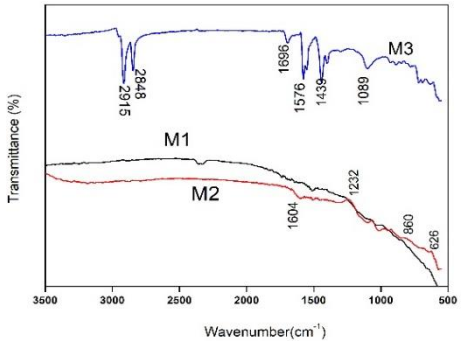

Fig. 4. FTIR spectra of M1, M2 and M3 MoS_2 samples.

The characteristic peaks at 1696 cm^{-1} and 1576 cm^{-1} were assigned to the symmetric $\upsilon(COO\text{-})_{symm}$ and asymmetric $\upsilon(COO\text{-})_{asymm}$ carboxylate group stretching band [18]. This signifies the surface modification of MoS_2 using Lithium Stearate. M3 confirms the attachment of stearate to the surface of the MoS_2 flakes which is expected to enhance the lipophilic property.

4.3. Raman Spectroscopy

Raman spectroscopy is the most important and powerful technique for the identification of two-dimensional MoS_2 materials, as the shift in peak positions could provide considerable information regarding the structure of these materials. The peak position gives additional information on the structure of 2D materials.

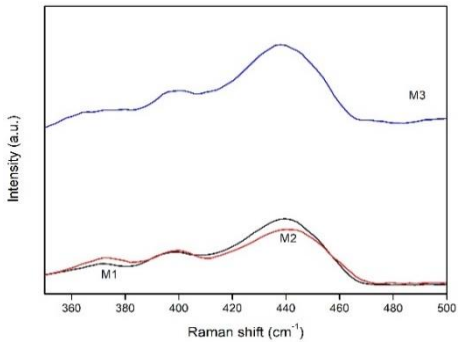

Fig. 5. Raman spectra of M1, M2 and M3 samples of MoS_2.

Fig. 5, shows the Raman spectra of M1, M2 and M3 MoS_2 material samples. M1 shows two peaks at 439 cm^{-1} and 397 cm^{-1} which were assigned to the high energy A_{1g} and the low energy E^1_{2g} vibrational modes respectively [19,20].

The A_{1g} mode indicates S atoms vibrating out of plane along C axis, whereas the E^1_{2g} mode represents the inter-layer distance displacements of Mo and S atoms respectively. For sample M2, moderate red shift in the E^1_{2g} and blue shift of A_{1g} peaks were observed, and the A_{1g} mode indicates out of plane of S atoms along C axis.

Accordingly, the phase shift can be attributed by using equation 4 as given below,

$$F(x) = A\sin(Bx - C) + D \tag{4}$$

where, A represents the amplitude, and C/B corresponds to the respective phase shifts.

The spectra for M3 sample showed combined blue-red shift in the E^1_{2g} and blue shift in the A_{1g} peaks of exfoliated MoS_2 sample (M2) with respect to the bulk MoS_2 sample (M1) [21,22]. Considering MoS_2 nanosheets, A_{1g} mode corresponds to the red-shift and signifies the decrease in inter-layer Van-der Waals force, and the E^1_{2g} mode represents long-range interlayer interactions of MoS_2 [23,24].

4.4. TGA Analysis

TGA analysis was carried out to study the influence of modifications of MoS_2 TGA curves for M1, M2 and M3 samples as shown in Fig. 6.

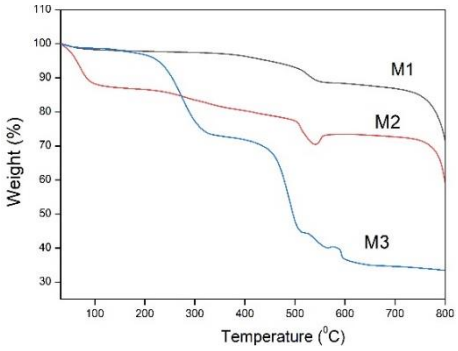

Fig. 6. Thermogravimetric analysis of M1, M2, M3 samples.

At first, M1 sample was accounted for TGA analysis. The material was subjected to TGA analysis from room temperature to 800^0C. Initially, from room temperature to 100^0C, the water content from the bulk material is being evaporated. Then, the sample was in a stable form from 100^0C to 378^0C. Subsequently, the sample was found to have weight loss around 10% due to the presence of Sulphur. Further, the sample was again seen to be stable for another 100^0C. Further, the sample was found to be influenced by a total weight loss.

The weight loss of the sample can be calculated by using equation 5 as given below,

$$\text{Weight loss } (\%) = \frac{m_i - m_t}{m_i} \times 100 \tag{5}$$

where, m_i corresponds to the initial mass and m_t represents the final mass of the sample.

M2 sample was seen to have a weight loss due to the presence of water content, and the weight loss was nearly 12%. The sample was gradually seen to have additional weight loss beyond 600^0C. The weight percentage was observed to dip to approximately zero. In M3 sample, the solid-state transformation (from solid to melted phase) was seen to occur at both 30^0C and 98^0C. The first transformation at 98^0C would be still endothermic, regardless of the presence of atmospheric temperature. In stagnant environments, lithium stearate undergoes oxidation in between 169^0C and 360^0C. The process is exothermic, meaning it releases loads of heat. Lithium oxalate was under inert atmosphere because the two liquids couldn't be separated. The acid decomposes to carbonate at 550^0C. A slight drop in initial degradation temperature of the composites shall be attributed to the early decomposition of intercalated and absorbed lithium stearate molecules [25].

4.5. SEM EDAX Analysis

The SEM image in Fig. 7(a) for sample M1 shows thick layers as expected for bulk MoS_2. Exfoliation samples' SEM images for M2 and M3 samples signified in Fig. 7(b)-7(c) indicates that the flake thickness got decreased, suggesting exfoliation. The corresponding EDAX spectra for samples M1, M2 and M3 were shown in Fig. 7(d)-7(f).

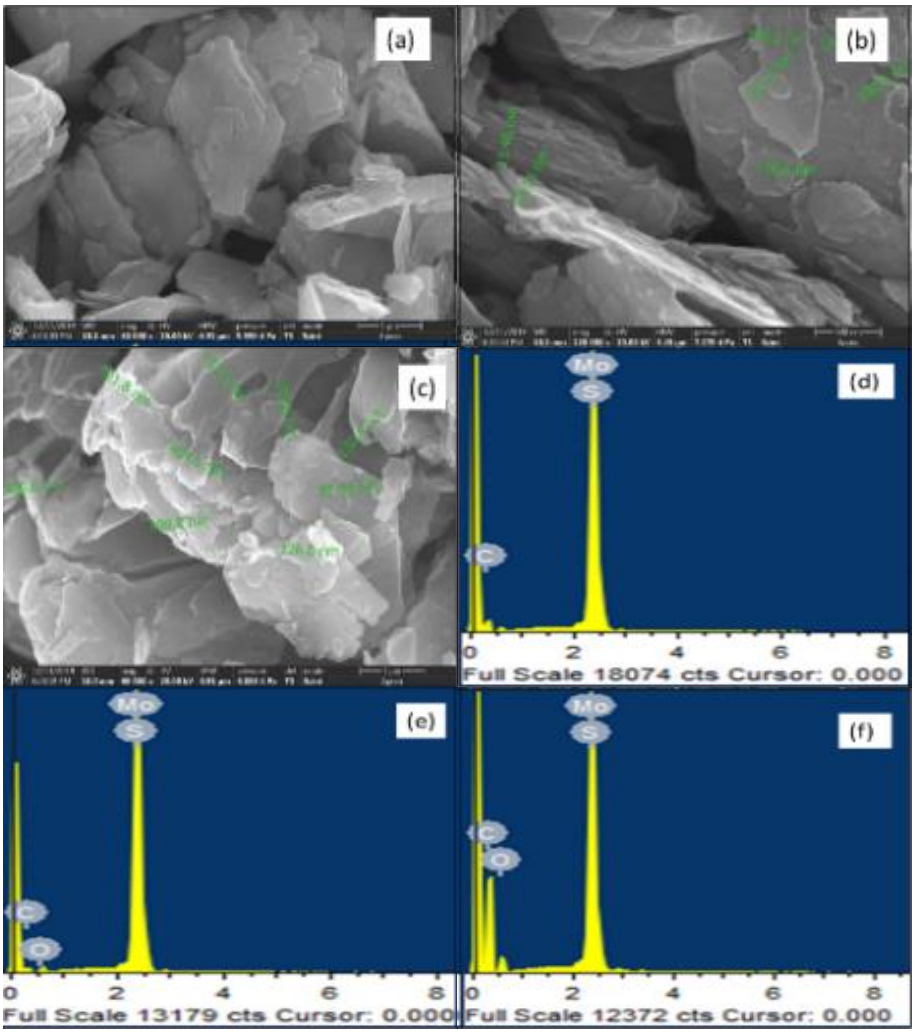

Fig. 7. SEM and EDAX images of M1 (a, d), M2 (b, e), M3 (c, f) samples of MoS_2.

Table 3. Concentration of elements in W% for samples M1, M2 and M3.

Elements	M1 (W%)	M2 (W%)	M3 (W%)
Carbon	41.21	23.32	67.23
Oxygen	_	7.04	8.51
Sulphur	20.04	23.23	8.76
Molybdenum	38.75	43.41	15.51

Table 3 shows the elemental concentration in weight percentage for all the three MoS_2 samples M1, M2 and M3. It was observed from Fig. 7(f) that, for sample M3, the Carbon and Oxygen peak concentrations got increased which in turn signifies the modifier influence on MoS_2. These results further signify the effectiveness of surface modification using stearate for sample M3.

5. Conclusion

In this paper, MoS_2 was successfully exfoliated and surface modified using lithium stearate as a novel modifier. The structural properties were studied from the XRD spectra. FTIR analysis confirmed the Stearate modification of MoS_2 surface which is expected to enhance the Lipophilic property. Raman analysis confirmed the sample exfoliation. The thermal stability of the modified sample could be understood from the TGA analysis. EDAX results clearly showed that the stearate surface treated MoS_2 samples exhibited an increase in Carbon and Oxygen elemental concentrations, which additionally confirms modification. The modifier and the material itself possess excellent lubricant properties facilitating lithium stearate assisted surface modification and exfoliation of Molybdenum disulfide to be a viable option in producing nanocomposites with distinct electrical properties, thereby making them largely applicable in numerous electrochemical energy storage devices including batteries and supercapacitors. In future, MoS_2 shall be exfoliated and surface modified using different related modifiers, so as to further analyze the surface modification process and its application in storage devices.

References

[1] T. D. Thangadurai, N. Manjubaashini, S. Thomas, H. J. Maria, Nanostructured Materials, Engineering Materials, Springer, 2020.
[2] A. Gana, H. Ben Temama, F. Lekminea, M. Naounc, O. Herzallaha, Digest Journal of Nanomaterials and Biostructures **16**(3), 815 (2021).
[3] H. O. A. Kareema, I. M. Ibrahimb, S. J. Mohameedc, F. J. Hameedd, Digest Journal of Nanomaterials and Biostructures **16**(2), 493 (2021).
[4] H. Deng, X. Liu, X. Jin et al., J Mater Sci: Mater Electron **32**, 9475 (2021).
[5] X. Jin, G. Li, J Mater Sci: Mater Electron **31**, 9377 (2020).
[6] R. B. Durairaj, S. Sivasaravanan, D. K. Sharma, S. Ramachandran, A. Heboyan, Digest Journal of Nanomaterials and Biostructures **16**(1), 161 (2021).
[7] M. N. Rizwan, A. R. Makhdoom, H. Farooq, M. A. Kalyar, I. M. Ghauri, Digest Journal of Nanomaterials and Biostructures **16**(1), 73 (2021).
[8] J. Yang, Q. Xiao, Z. Lin et al., Friction **9**, 1150 (2021).
[9] R. Hu, Z. Huang, B. Wang et al., J Mater Sci: Mater Electron **32**, 7237 (2021).
[10] L. Huang, L. Xu, Y. Yang et al., J Mater Sci: Mater Electron **31**, 6607 (2020).
[11] M. Zhao, L. Liu, B. Zhang, M. Sun, X. Zhang, X. Zhang, L. Wang, RSC Advances **8**(61), 35170 (2018).
[12] Y. Liu, X. He, D. Hanlon, A. Harvey, J. N. Coleman, Y. Li, ACS Nano **10**(9), 8821 (2016).
[13] D. Pradhan, J. P. Kar, Silicon (2021).
[14] M. Subitha, S. M. Sasikanth, B. Bindhu, Ionic liquid assisted exfoliation and dispersion of molybdenum disulphide: Synthesis and characterization, 2019.
[15] X. Ding, G. Fan, Y. Huang et al., J Mater Sci: Mater Electron **32**, 9640 (2021).
[16] M. G. Reddy, S. A. Shehzad, Appl. Math. Mech.-Engl. Ed. **42**, 541 (2021).
[17] K. Ren, Z. Liu, T. Wei et al., Nano-Micro Lett. **13**, 129 (2021).
[18] N. Ranjan, R. C. Shende, M. Kamaraj et al., Friction **9**, 273 (2021).
[19] L. Ma, G. Huang, W. Chen, Z. Wang, J. Ye, H. Li, J. Y. Lee, Journal of Power Sources **264**, 262 (2014).
[20] S. Geng, F. Tian, M. Li et al., Nano Res. (2021).
[21] H. S. S. Ramakrishna Matte, A. Gomathi, A. K. Manna, D. J. Late, R. Datta, S. K. Pati, C. N. R. Rao, Angewandte Chemie International Edition **49**(24), 4059 (2010).
[22] M. H. Köhler, J. P. K. Abal, G. V. Soares, M. C. Barbosa, Das R. (eds) Two-Dimensional (2D) Nanomaterials in Separation Science. Springer Series on Polymer and Composite Materials, Springer, 2021.
[23] M. Kremser, M. Brotons-Gisbert, J. Knörzer et al., NPJ 2D Mater Appl **4**, 8 (2020).
[24] I. Paradisanos, S. Shree, A. George et al., Nat Commun **11**, 2391 (2020).
[25] M. M. Barbooti, D. A. Al-Sammerrai, Journal of Thermal Analysis **30**(3), 587 (1985).